HAL
open science

Alachlor dechlorination prior to an electro-Fenton process Influence on the biodegradability of the treated solution

Y.-Y. Lou, F. Geneste, I. Soutrel, A. Amrane, F. Fourcade

To cite this version:

Y.-Y. Lou, F. Geneste, I. Soutrel, A. Amrane, F. Fourcade. Alachlor dechlorination prior to an electro-Fenton process Influence on the biodegradability of the treated solution. Separation and Purification Technology, 2020, 232, pp.115936. 10.1016/j.seppur.2019.115936 . hal-02281864

HAL Id: hal-02281864

https://univ-rennes.hal.science/hal-02281864v1

Submitted on 16 Dec 2019

HAL is a multi-disciplinary open access archive for the deposit and dissemination of scientific research documents, whether they are published or not. The documents may come from teaching and research institutions in France or abroad, or from public or private research centers.

L'archive ouverte pluridisciplinaire **HAL**, est destinée au dépôt et à la diffusion de documents scientifiques de niveau recherche, publiés ou non, émanant des établissements d'enseignement et de recherche français ou étrangers, des laboratoires publics ou privés.

Alachlor dechlorination prior to an electro-Fenton process: Influence on the biodegradability of the treated solution

Yao-Yin Lou[a,b], F. Geneste[a], I. Soutrel[b], A. Amrane[b], F. Fourcade*[b]

[a] Univ Rennes, CNRS, ISCR [(Institut des Sciences Chimiques de Rennes)] – UMR 6226, F-35000 Rennes, France

[b] Univ Rennes, Ecole Nationale Supérieure de Chimie de Rennes, CNRS, ISCR [(Institut des Sciences Chimiques de Rennes)] – UMR 6226, F-35000 Rennes, France

Abstract

This study investigates alachlor herbicide removal by electro-Fenton (EF) process with and without a previous dechlorination step by electro-reduction (ER-EF). The objective is to evaluate the relevance of dechlorination before electro-Fenton according to the biodegradability evolution and the energy consumption. The influence of the applied current, the ferrous ions concentration and the air flow rate on the production of hydrogen peroxide and on the general behavior of alachlor removal by EF oxidation was studied and optimized EF conditions were chosen. Scavenger tests were performed to determine the contribution of hydroxyl radicals (•OH), superoxide radicals ($•O_2^-$) and sulfate radicals ($•SO_4^-$) during alachlor degradation. Some intermediate products formed during degradation by EF of alachlor and of the electroreduced solution were identified and the evolution of small organic acids was examined. Possible pathways of alachlor degradation and of deschloroalachlor, the mean byproduct from ER, were proposed on the basis of the EF reaction. EF treatment significantly improved the biodegradability of electrolyzed solutions with BOD_5/COD ratio increasing from 0 to 0.4 after 0.5 h oxidation and can be further enhanced by the application of ER prior to EF, leading to a maximum value for the BOD_5/COD ratio of 0.7 that can be due to the absence of chloroacetic acid found during the EF treatment. The energy consumption of the different electrochemical processes was also evaluated.

Keywords: Alachlor; Electro-Fenton; Electro-reduction; Biodegradability, combined processes

Accepted manuscript

1 Introduction

Alachlor, 2-chloro-(2',6'-diethyl-*N*-(methoxymethyl)acetanilide), has been one of the mostly used herbicides to remove annual grasses and broadleaf weeds and promote crops yield in the last few decades [1, 2]. The excess use of alachlor has led to contaminations in surface water and farming soil [3]. Alachlor and some of its metabolites have also been detected in *vitro* in human liver microsomes and in urine [4, 5]. To avoid this potential threat to human *via* drinking water, alachlor has a maximum contaminant level of 2.0 μg L^{-1} set by US EPA [6]. More strict control at 0.1 μg L^{-1} for any particular pesticides is regulated by the European Union (European Union, 2007).

Considering its high toxicity and poor biodegradability, alachlor negatively impacts the activity of the activated sludge, which indicates the unfeasibility of utilizing municipal sewage treatment process to treat wastewaters containing alachlor [7]. It has been shown that the presence of chlorine atoms in the chlorinated organic compounds structure is considered to be the main cause of their toxic properties [8]. To reduce toxicity, electro-reduction (ER) has been chosen as a pretreatment before the biological process because of its high selectivity of dechlorination on catalyst-modified cathodes, which can enhance the pollutants biodegradability [9, 10]. Hence, some previous works about ER pretreatment of alachlor have been attempted, including Co complex-supported catalyst [11, 12] and nanoparticle Ag-modified electrodes [13, 14]. After ER pretreatment on nanoparticle Ag-modified cathode, alachlor has been completely degraded with a dechlorination yield of 77% and its dechlorinated derivative (deschloroalachlor) has been formed with a yield of 65%. Higher selectivity toward the dechlorination process has been obtained on Co-complex-modified cathode with a dechlorination yield of 95% and 86% yield of deschloroalachlor. However, BOD_5 measurements have shown that the main by-product deschloroalachlor is also not biodegradable [11]. This result is in accordance with the work of Zhang et al. [15] who found that the amide nitrogen's alkoxymethyl group in chloroacetamide organics influences significantly and negatively their biodegradability. Therefore, some other technologies that can degrade the amide nitrogen's alkoxymethyl group are necessary.

Accepted manuscript

Various kinds of techniques have been put forward to remove alachlor from aquatic environment. Advanced oxidation processes (AOPs) have attracted considerable interests owing to the generated reactive oxidant radicals •OH, especially the Fenton reaction (equation (1)) combined with UV [16] or sonication [17], the peroxone process [18], photocatalysis [3, 19, 20] and electrochemical processes [21]. Among AOPs, electro-Fenton (EF) was considered in this study because of its advantage of self-generation of H_2O_2 by reduction of O_2 (E° = 0.695 V/SHE), as shown in equation (2), which avoids the transportation and storage of H_2O_2.

$$Fe^{2+} + H_2O_2 \rightarrow Fe^{3+} + \cdot OH + OH^- \quad (1)$$

$$O_2 + 2H^+ + 2e^- \rightarrow H_2O_2 \quad (2)$$

Instead of complete mineralization, the partial oxidation of toxic compounds by EF can be used to enhance biodegradability cost [22-25], in order to save energy and decrease the treatment cost. In this work, a succession of ER and EF was considered as a pretreatment prior to a cost-efficiency biological treatment. The first objective of this combined system is to avoid the formation of short-chain chlorinated alkane species and carboxylic acids, which have resistance to oxidation by the Fenton reaction and may flow into the biological process and hinder the activity of micro-organisms [26]. The comparison of EF with the combination of ER and EF in terms of improvement of alachlor biodegradability and energy consumption was performed. We first optimized the EF parameters such as current, ferrous concentration and air flow rate. To go further in the understanding of the mechanism involved and the by-products formed, the radicals contribution was also examined by scavenger tests and the formation of high-molecular-weight (HMW) degradation by-products and low-molecular-weight by-products, including small organic acids and inorganic anions, was studied. The biodegradability improvement in different conditions of electrochemical treatment was also evaluated.

Accepted manuscript

2 Materials and Methods

2.1 Chemicals products

All chemicals used were of analytical grade and used without further purification. Alachlor, deschloroalachlor, ferrous sulfate ($FeSO_4$), sodium hydroxide (NaOH) and sulfuric acid (H_2SO_4) were obtained from Sigma-Aldrich. The initial pH of the solutions was adjusted to 3 by adding analytical grade H_2SO_4 purchased from Acros Organics. Anhydrous sodium sulfate (Na_2SO_4) was from Acros Organics. Isopropyl alcohol (IPA, $(CH_3)_2CHOH$, >99.5%), tertbutyl alcohol (TBA, $(CH_3)_3OH$, >99.0%) and 1, 4-benzoquinone (BQ, $C_6H_4O_2$, >97%) were purchased from Sigma-Aldrich. Acetonitrile (HPLC-grade) was purchased from Fisher Scientific (Loughborough, UK). Ultra-pure water obtained from ELGA Purelab Option-Q DV 25 system was utilized for the preparation of all working solutions, as well as HPLC and LC–MS/MS mobile phases.

2.2. Electrochemical process

The electrodechlorination processes were conducted as described in our previous work [13, 14, 27] modified as follow: 25 mL alachlor (50 mg L^{-1}) was electro-dechlorinated on a homemade electrochemical cell with a Ni layer covered support modified by Ag nanoparticles as the cathode (volume: 0.13 cm^3), at -1.6 $V/_{MSE}$ in 0.05 mol L^{-1} NaOH. Then the pH of the electrolyzed solution (named as $solution^{ER}$) was adjusted to 3 for the subsequent EF treatment and then to 7 for the biodegradability estimation and the biological treatment. The EF experiments were performed at ambient temperature in an undivided cylindrical glass cell containing 250 mL of $solution^{ER}$ or of a solution of 50 mg L^{-1} alachlor (named as $solution^{alachlor}$) in 0.1 mol L^{-1} Na_2SO_4 . The cell was equipped with two electrodes: one 3-dimensional graphite felt (GF) piece (8.5 cm × 5.0 cm × 1.0 cm) as cathode (Mersen; Paris La Defense, France) and a cylindrical platinum (Pt) electrode (34.6 cm^2) as anode. Continuous saturation of O_2 was ensured by bubbling compressed air flow rate of 0.1-0.5 liter per minute, starting 20 min before electrolysis. The EF process was conducted in galvanostatic mode at a current in the range 15-300 mA, with a ferrous ions solution in the range 0-1.0 mmol L^{-1} at pH 3.0 adjusted with H_2SO_4. A pH value of 3.0 was

Accepted manuscript

chosen, because it has been shown to be the optimal pH for the Fenton's reaction [28]. All solutions were vigorously stirred (300 rpm) with a magnetic bar during treatment.

2.3. Biodegradability estimation

Biochemical oxygen demand in 5 days (BOD_5) was considered to evaluate the biodegradability of the studied solutions [29]. BOD_5 measurements were carried out in NANOCOLOR® BOD_5-TT test tubes (from Macherey-Nagel, German) at 20.0±0.5^{o}C, pH 7 and in obscurity during 5 days. For inoculation, an initial activated sludge concentration of 0.05 g L^{-1} was targeted. A control sample containing 150 mg L^{-1} glutamic acid and glucose known as biodegradable compounds was conducted to check the viability of the activity sludge. A blank solution containing pure water was performed to deduce the biochemical oxygen demand corresponding to the endogeneous respiration. 120 µL of a mineral solution was also added, containing 5.625 g L^{-1} $MgSO_4 \cdot 7H_2O$, 6.875 g L^{-1} $CaCl_2$, 0.375 g L^{-1} $FeCl_3$, 0.5 g L^{-1} NH_4Cl. BOD_5/COD value was introduced to evaluate solutions' biodegradability. Above a threshold value of 0.4, the solution is considered as easily biodegradable [29].

2.4 Biological treatment

Biological treatments were conducted in duplicate for 21 days at 25C^o and in 500 mL Erlenmeyer flasks containing 250 mL solution, magnetically stirred at 200 rpm, closed by a cellulose cap to guarrantee oxygenation. Activated sludge was inoculated to achieve an initial concentration of 0.5 g L^{-1}.The following mineral solution was added (mg L^{-1}): K_2HPO_4, 208; KH_2PO_4, 85; $Na_2HPO_4 \cdot 2H_2O$, 154.4; $MgSO_4 \cdot 7H_2O$, 22.6; $CaCl_2$, 27.6; $FeCl_3$, 0.26; NH_4Cl, 75. A control test with sterilized sludge was performed to determine the biosorption effect during the biological treatment. The pH of all solutions were adjusted to 6-8 with 0.1 M H_2SO_4 and NaOH. Samples were taken regularly for TOC and HPLC analyses after a filtration on a 0.45 µm membrane.

2.5. Analytical procedures

2.5.1. HPLC analysis

Accepted manuscript

The measurements of the alachlor and deschloroalachlor concentrations were performed by a Waters High Performance Liquid Chromatography (HPLC) system consisting of a Waters™ 600 instrument, equipped with a C18 reverse-phase Column (4.6 mm × 250 mm, 5 μm), along with a 996 Photodiode array detector and a Waters 717 plus Autosampler injector. The system was controlled through an Empower program. Prior to analysis, the samples had to be filtered through a 0.22 μm filter. The injection volume was set at 10 μL and an isocratic eluent Water/Acetonitrile (60/40) was pumped at a flow rate of 1 mL min^{-1}. Alachlor and deschloroalachlor had retention times of 2.65 and 2.33 min, respectively. Under these conditions, many peaks of the byproducts appeared at lower retention times. Detection was performed with a photodiode array detector Waters 996 at 196 nm.

2.5.2. UPLC-MS analysis

To identify the by-products obtained during the alachlor and the electroreduced solution degradation, several samples were analyzed by ultra-high pressure liquid chromatography (Acquity UPLC – Waters) coupled to mass spectrometry Tandem (Triple Quad Quattro Premier Waters). The analytes were separated by the Waters Acquity UPLC system consisting of an Acquity UPLC binary solvent manager, an Acquity UPLC sample manager and an Acquity UPLC column heater equipped with a Waters Acquity UPLC BEH C18 column (2.1 × 100 mm, 1.7 μm particle size) (Milford, MA, USA). Isocratic LC elution was performed with acetonitrile quality LC-MS as mobile phase A and an ultrapure water 9:1 acetonitrile (v/v) mixture as mobile phase B. Separation of the analytes on the column was performed at 0.4 mL min^{-1} flow rate.

2.5.3. Other analytical methods

NH_4^+-N, and NO_3^--N were measured *via* colorimetric methods (APHA) using a UV-visible spectrophotometer (DR5000, HACH, Colorado) [30]. The mineralization of the organic compounds was monitored by measuring the non-purgeable organic carbon (NPOC) abatement by TOC-VCPH/CPN Total Organic Carbon Analyzer Schimadzu. The hydrogen peroxide (H_2O_2) concentration was measured by titration with a solution of sodium thiosulfate ($Na_2S_2O_3$) [31]. Chemical oxygen demand (COD) was determined using NANOCOLOR® COD 160 kit (from Macherey-Nagel, Germany). Low-molecular-weight

Accepted manuscript

organic acid and inorganic anions were quantified by ion exclusion chromatography using a Dionex 900 ion chromatograph (IC, Thermo, USA) equipped with a conductivity detector. An Ionpac (4 mm × 250 mm) was used as anion exchange column. The eluent was ultra-pure water at a flow rate of 1.0 mL min^{-1}.

3. Results and discussion

3.1. Optimization of the EF oxidation

3.1.1. Effect of the current

The current is a key parameter that influences the EF process [28, 32]. To find the optimal current to be applied, cathodic current from -15 to -300 mA were investigated. Current of -30 mA corresponded to a potential around -0.5 $V/_{SCE}$ in our experimental system (data not shown), which is the theoretical optimal cathodic potential for the generation of H_2O_2 [33]. A maximum accumulated H_2O_2 concentration of 5.92 ± 0.33 mmol L^{-1} was obtained at a current of -200 mA after 3 h of electrolysis, as shown in Figure 1(a). According to equation (2), a more negative current is expected to improve the production of H_2O_2 [34] at the cathode and the production of hydroxyl radicals at the Pt anode (Pt($^{\bullet}$OH)) [35, 36]. However, beyond -200 mA, the opposite trend was observed. It can be explained by the competition with the four-electron reduction of O_2 (E° = 1.229 V/SHE), the reduction of H_2O_2 into H_2O (E° = 1.763 V/SHE), and the hydrogen evolution reaction (E° = 0 V/SHE) which are favored when a high current density is used as shown in equation (3), (4) and (5) [37-40]. Meanwhile, an enhanced current could promote parasitic reactions at the anode, according to equations (6) (E°= 1.440 V/SHE) and (7) [41], leading to the consumption of H_2O_2.

$$O_2 + 4H^+ + 4e^- \rightarrow 2H_2O \quad (3)$$

$$H_2O_2 + 2H^+ + 2e^- \rightarrow 2H_2O \quad (4)$$

$$2H_3O^+ + 2e^- \rightarrow H_2 + 2H_2O \quad (5)$$

$$H_2O_2 \rightarrow HO_2\bullet + H^+ + e^- \quad (6)$$

$$HO_2\bullet \rightarrow O_{2(g)} + H^+ + e^- \quad (7)$$

Accepted manuscript

Oxidant radicals, such as •OH, are produced by the activation of the electro-generated H_2O_2 in the presence of the ferrous catalyst (equation (1)). Consequently, an increase of the applied current led to a significant enhancement of the kinetic of alachlor removal and mineralization (Figures 1(b) and 1(c)). However and according to the maximum amount of H_2O_2 electro-generated, maximum degradation and mineralization yields were obtained for an applied current of -200 mA and 0.1 mM of ferrous ions concentration. It can be observed that both the removal of the herbicide and the mineralization were found to follow a pseudo-first order kinetic model with maximum kinetic rate constants (k_{app}) of 0.451 ± 0.09 min^{-1} (Supplementary material Table S1) and 0.0137 ± 0.0007 min^{-1} (Supplementary material Table S2), respectively. Hence, as discussed above, the optimal applied current of -200 mA was selected and considered thereafter.

3.1.2. Effect of the ferrous ions concentration

The effect of Fe(II) concentration on the degradation of the target molecule was investigated in the presence of 50 mg L^{-1} of alachlor and for an applied constant current of -200 mA; the corresponding results are displayed in Figure 2. According to our previous work on the degradation of enoxacin [42] and metronidazole [25], the optimal Fe(II) concentration is around 0.1-0.2 mmol L^{-1}. Hence, a range of Fe(II) concentrations, from 0.02 to 1.0 mmol L^{-1}, was investigated in this study. The percentage of alachlor conversion increased with the catalyst concentration up to 100% within 10 min EF oxidation, as shown in Figure 2(a). It should be observed that increasing the catalyst concentration beyond 0.05 mmol L^{-1} did not have a significant impact on the degradation rate. The alachlor degradation versus time followed a pseudo-first order kinetic model with increased k_{app} from 0.033 ± 0.002 min^{-1} to 0.56 ± 0.07 min^{-1} as Fe(II) concentration increased from 0.02 to 0.1 mmol L^{-1} (Supplementary material Table S1). On the other hand, alachlor degradation was also observed in the absence of Fe(II), with 77.3% degradation after 1 h electrolysis, showing the contribution of the electrochemical oxidation at the Pt anode or/and reduction on graphite felt to alachlor degradation. Indeed, it was previously shown that alachlor can be reduced to deschloroalachlor on graphite felt electrode [12]. Moreover, a reaction between alachlor and the produced hydrogen peroxide can also occur in solution [43]. Maximum mineralization yield was 91.8 ± 0.8%, obtained for 0.05 mmol L^{-1} Fe(II)

Accepted manuscript

within 3 h EF oxidation, as shown in Figure 2(b). The low mineralization observed in the absence of the ferrous catalyst (Figure 2(b)) suggested that radicals are the main contributors in the mineralization of alachlor. The negative effect of the Fe(II) amount beyond 0.1 mmol L^{-1} should be most likely attributed to a competitive reaction occurring between the •OH generated and the excess of Fe(II) according to equation (8) with a rate constant of 3.2 10^8 L mol^{-1} s^{-1} [41, 42]. [44]. As for target compound degradation, mineralization also followed a pseudo first order kinetic model, and maximum k_{app} was found to be 0.014 ± 0.002 min^{-1} for a Fe(II) concentration of 0.05 mmol L^{-1}. As a result, 0.05 mmol L^{-1} was the optimal catalyst concentration and was considered thereafter.

$$Fe^{2+} + \bullet OH \rightarrow Fe^{3+} + OH^- \quad (8)$$

3.1.3. Effect of the air flow rate

The conductive air pump does not only provide sufficient dissolved O_2 for electrogeneration of H_2O_2 but also enhances the mass transfer; so that the air flow rate is also an interesting parameter to be investigated. As illustrated in Figure 3(a), the accumulated H_2O_2 reached a maximum of 3.56 ± 0.06 mmol L^{-1} for an air flow rate of 0.3 L min^{-1}, compared to 0.1 and 0.5 L min^{-1}. Although the air flow rate did not show significant influence on dissolved O_2 (DO) content, which was 7.1 ± 0.6 mg L^{-1} (close to the limit of solubility of O_2 in water, which is around 9 mg L^{-1} at 20 °C) for all flow rates, increasing the air flow rate enhances the mass transfer in the solution. However, over-pumped air could result in an excessive production of bubbles, leading to a heterogeneous distribution of current density inside the graphite felt and to an increase in the electric resistance. This phenomenon would explain the decrease of the H_2O_2 concentration when an air flow rate of 0.5 L min^{-1} was used. Indeed, a potential around -1.5 $V/_{SCE}$ was measured at the working electrode for a flow rate of 0.5 L min^{-1}. At this potential, the four-electron reduction of O_2 (equation (3)) becomes predominant, decreasing the amount of formed H_2O_2. Another side-reaction that could occur at -1.5 $V/_{SCE}$ is the decomposition of H_2O_2 into water, according to equation (4) [28, 40]. For lower air flow rates, the potential was found to be -0.75 $V/_{SCE}$, which is in favor of H_2O_2 formation. Similarly, Zhou et al. [40] have observed 10% decrease of the accumulated H_2O_2 in the EF process with hydrazine hydrate chemically modified graphite felt as the cathode after increasing the O_2 flow rate

Accepted manuscript

from 0.4 to 0.6 L min^{-1} and found that the optimal potential to form H_2O_2 was -0.75 $V/_{SCE}$. H_2O_2 also became easily decomposed into water in the case of 0.5 L min^{-1}, according to equation (4). For 0.1, 0.3, and 0.5 L min^{-1}, mineralization yields were 84% ± 4%, 92% ± 2% and 82% ± 2%, respectively, after 3 h EF (Figure 3(c)). The mineralization followed a pseudo first order kinetic model with k_{app} values of 0.013 ± 0.001 min^{-1}, 0.014 ± 0.002 min^{-1} and 0.009 ± 0.001 min^{-1} for 0.1, 0.3 and 0.5 L min^{-1}, respectively (Supplementary material Table S2). Alachlor degradation increased with the air flow rate up to 100% within 10 min EF oxidation, as shown in Figure 3(b). The alachlor degradation with time followed a pseudo-first order kinetic model with increased k_{app} from 0.19 ± 0.09 min^{-1} to 0.54 ± 0.07 min^{-1} as air flow rate increased from 0.1 to 0.5 L min^{-1} (Supplementary material Table S1). From the above results, 0.3 L min^{-1} was therefore chosen as the optimal air flow rate and was therefore considered thereafter. If the mineralization yield was in accordance with the hydrogen peroxide production, the behavior of the degradation yield was different since it increased from 0.1 to 0.5 L min^{-1}. If the electrochemical reaction of alachlor at the electrode surface is mainly responsible for its degradation, an increase of air flow rate and then a better mass transport of alachlor toward the electrode surface could explain this trend.

3.2. Possible mechanism of alachlor degradation

3.2.1. By-products identification

LC/MS analysis was considered to investigate the intermediates generated during EF oxidation of pure alachlor and of the electroreduced solution. In order to identify a maximum of intermediates, the EF oxidations were performed at 50 mA. In total, 18 aromatic and/or cyclic molecules were identified as the primary transformation by-products (compounds **2** to **11** for alachlor and compounds **12** to **19** for the electroreduced solution considering deschloroalachlor as the main product of alachlor dehalogenation) (Supplementary material Table S3 and Table S4).

3.2.1.1. Alachlor oxidation

On the basis of these intermediates and the related literatures [16, 18, 20, 21, 45-47], we proposed that alachlor degradation mechanism involved alkylic oxidation, cleavage of C-N, C-Cl, C-O, and/or C-C bonds, cyclization, and dealkylation (Figure 4). First, compound

Accepted manuscript

2 was generated by dealkylation of alachlor upon the attack by •OH and then further oxidized to compounds **6** and **5** by scission of the R-N bond and hydroxylation, as it has been previously observed in photo-Fenton oxidation [16]. Compound **9** would be generated from compound **5** by dehalogenation and dealkylation. Subsequently, cyclization of compounds **2** and **6** generate heterocyclic compounds **10** and **11** with one aromatic ring, respectively, as it has been also identified in O_3/H_2O_2 treatment [18]. In the meantime, compound **3** was formed by direct scission of the C-Cl bond of alachlor, and was further oxidized to compounds **8** and **7**, as reported in other AOPs [18, 45, 46]. The cleavage of the C-N bond occurring by α/β scission of the bond and hydroxylation generate compound **4**, which could be oxidized *via* the further cleavage of the C-Cl bond and hydrogen abstraction to form **8**, as also reported in BDD(•OH) oxidation [21]. The last step involved oxidative opening of the aromatic ring, leading to small organic ions and inorganic species.

3.2.1.2. Deschloroalachlor oxidation

As deschloroalachlor was the main by-product of alachlor electroreduction, compounds identified after oxidation of the electroreduced solution were considered as intermediates of deschloroalachlor. The mechanism suggested from the by-products identification showed high similarities with those of alachlor (Figure 5). For example, the compound **13** corresponded to compound **2** without chlorine. The compound **15** was structurally closed to the compound **5**. The compound **10** was identified during the oxidation of alachlor and during the oxidation of the electroreduced solution. The compound **16** was already identified by Pipi et al. [21] in their study on alachlor oxidation. These high similarities between the identified by-products showed that the two mechanisms were analogous and that the presence of a chlorine atom in the molecule did not change the sites of radical attack.

3.2.2. Inorganic ions evolution

From the above results, optimal alachlor degradation (100% conversion within 15 min) and mineralization (over 90% after 180 min) can be reached in the following conditions (named as opt-condition): a current of 200 mA, in the presence of 0.05 mmol L^{-1} of Fe(II) catalyst, with an air oxygen rate of 0.3 L min^{-1}. EF treatment was performed in these optimal

Accepted manuscript

conditions for the non-pretreated alachlor solution (solution^{alachlor}) and an electroreduced solution of alachlor (solution$^{alachlor\text{-}ER}$) prior to biodegradability evaluation.

Ions chromatography (IC) was then used to identify and quantify the low-molecular-weight organic acids and inorganic anions generated during the alachlor degradation process (Figure 6). The concentrations of Cl^-, NH_4^+, and NO_3^- were monitored during EF process; while NO_2^- was not detected. The release of chloride ions and nitrogenous ions at the early stages of the electrolysis proved that alachlor was readily removed in the EF process and that previously identified intermediates were decomposed quickly. A significant decrease of the total nitrogen was detected after 0.5 h, along with NH_4^+ concentration decrease after 0.5 h and NO_3^- concentration decrease after 1.5 h. The decrease of the total nitrogen content could be explained by the release of N_2 after the oxidation of NH_4^+ into NO_3^- [21, 48]. After 2h of electrolysis, the concentration of chloride ions reached 99% ± 8%, showing that alachlor was totally dechlorinated. The slight decrease of the percentage in solution to 91% ± 7% after 3h of electrolysis was not significant regarding the measurement uncertainties. The increase of the nitrogen from NH_4^+ and NO_3^-, which reached a maximum after 0.5h of EF treatment, was faster than the increase of Cl^- content. This suggested that the cleavage of the C-N bond occurred prior to the scission of the C-Cl bond, leading to the formation of organo-chloride intermediates in solution.

3.2.3. Contribution of free radicals to alachlor mineralization

The reactive oxidants, which could be formed during the EF process, are •OH and/or superoxide radicals ($•O_2^-$), the conjugate base of peroxide radicals ($HO_2•$) ($HO_2• \leftrightarrow H^+ + •O_2^-$), and/or sulfate radical $•SO_4^-$ thanks to •OH oxidation ($•OH + SO_4^{2-} \rightarrow HO^- + •SO_4^-$) [49]. The role of radicals involved in the EF process was determined using three radical scavengers, including isopropyl alcohol IPA (•OH and $•SO_4^-$ scavenger), tert-butyl alcohol TBA (•OH scavenger, but not for $•SO_4^-$) and benzoquinone BQ ($•O_2^-$ scavenger) [50]. A control test was also performed in the absence of Fe(II) in order to determine the electrooxidation or/and electroreduction contribution, and the results are presented in Figure 7. In the optimal conditions (previously named as 'opt-condition'), alachlor conversion was almost 100% within 15 min. 89% ± 2% alachlor conversion was obtained

Accepted manuscript

within 15 min in the presence of BQ indicated that 11% of alachlor conversion can be attributed to the oxidation by $\bullet O_2^-$ / $\bullet HO_2^-$. When TBA was added in the solution, alachlor conversion was only 20.6 % ± 0.5% within 15 min instead of 99%, underlining the important role of • OH in the degradation process. The comparison between the experiments performed with TBA and IPA after 60 min, showed a contribution to alachlor conversion of 63% and 12% for •OH and $\bullet SO_4^-$ radicals, respectively. Without Fe(II) catalyst, only 81% ± 5% alachlor conversion after 60 min and 15.2% ± 0.5% mineralization after 3 h were obtained. Since a possible reaction between alachlor and hydrogen peroxide can occur in solution [43], the presence of deschloroalachlor (19.68 mg L^{-1} at 100 min) indicated that alachlor underwent electroreduction on the graphite felt in these conditions (Supplementary material Figure S1). The Direct oxidation of alachlor did not take place on the Pt anode since no signal for alachlor oxidation was observed by cyclic voltammetry (Data not shown). According to these results, •OH was the main radical species involved in the alachlor degradation.

3.3. Comparison of the EF process with the coupling of electroreduction and electro-Fenton treatment (ER-EF)

3.3.1. Biodegradability and biodegradation of alachlor before and after electroreduction

An efficient method to evaluate the biodegradability of a solution is to use the ratio of Biological Oxygen Demand (BOD_5) and Carbon Oxygen Demand (COD) over 5 days. Indeed, it has been demonstrated that an effluent can be considered as easily biodegradable if its BOD_5/COD ratio is above 0.4 [51]. We have previously reported that this ratio was lower than 0.02 after electroreduction of alachlor on Ni foams modified with Ag nanoparticles [14]. To go further in the biodegradability estimation of alachlor solution after ER ($solution^{alachlor\text{-}ER}$), a biological treatment was implemented during 21 days with pure alachlor ($solution^{alachlor}$) and with the $solution^{alachlor\text{-}ER}$. Whereas, the $solution^{alachlor}$ did not show any increase of the mineralization yield, a value of 46% was obtained for the $solution^{alachlor\text{-}ER}$ after one day of culture, indicating the presence of some biodegradable by-products generated during the ER process (Figure S2(a)). A control test with sterilized sludge was performed to assess for possible biosorption of the $solution^{alachlor\text{-}ER}$ during the

Accepted manuscript

setout of culture (Figure S2(b)). About 11% TOC decrease can be attributed to the biosorption onto activated sludge and hence 35% of mineralization corresponded to the biodegradation of the by-products from ER. However, as observed in Figure S2(c), a constant concentration of alachlor in solution^{alachlor} and deschloroalachlor in solution$^{alachlor-ER}$ were observed during the 21 days of culture, confirming that alachlor and deschloroalachlor were biocalcitrant.

3.3.2. Biodegradability improvement with electro-Fenton

The evolution of biodegradability was then examined thanks to the BOD_5/COD ratio during the EF treatment of a solution^{alachlor} and a solution$^{alachlor-ER}$. In both cases, the initial biodegradability was negligible and increased with the EF oxidation time, showing a significant biodegradability improvement by the EF process. Moreover, biodegradability was often higher with the solution resulting from the combination of ER and EF (ER-EF treatment), compared to EF alone (Table 1). This indicates that ER pretreatment had an impact on biodegradability improvement. The highest biodegradability was observed after 1 h of oxidation, with BOD_5/COD ratios of 0.65 and 0.70, for EF and ER-EF treatments, respectively. The decrease of biodegradability after 1 h of oxidation could be explained by about 50% decrease of available organic carbon source for microorganisms.

Interestingly, after 0.25h of oxidation, the BOD_5/COD value increased to 0.16 for the ER-EF treatment whereas it was still not measurable for EF. This could be explained by the presence of organo-chlorinated compounds after 0.25h of EF treatment since 40% of the chlorine from alachlor were found as Cl^- ions in solution against 80% for the combined process (Figure 8a). This is in agreement with the study on the suggested EF mechanism, which underlined a preference for a radical attack of the C-N and C-O bonds instead of the C-Cl bond. This phenomenon is likely to results in the formation of organo-chlorinated compounds. Higher TOC values were observed in the case of the coupling of ER and EF. The presence of a higher concentration of Cl^- in the solution$^{alachlor-ER}$ could lowered the efficiency of the EF process, since Cl^- has a scavenging effect on •OH (equations (8) and (9)) [49, 50]. As a result of higher TOC values, higher organic carbon remained available for microbial growth.

Accepted manuscript

$$\bullet OH + Cl^- \rightarrow \bullet ClOH^- \quad (8)$$

$$\bullet ClOH^- + Cl^- \rightarrow \bullet Cl_2^- + OH^- \quad (9)$$

Acetic, formic and oxalic acids were analyzed (Figure 8b) since they are low-molecular-weight organic acids known to be formed during EF treatment and to be beneficial to microbial growth [42]. Acetic acid is oxidized to oxalic and formic acids which are directly transformed into CO_2 [52].The significant higher content of these organic acids for the ER-EF treatment, compared to the EF treatment, is probably related to the better biodegradability obtained. Furthermore, these organic acids do not easily react with radicals, which also partly accounted for the higher TOC values observed in ER- EF treatment [26].

For the EF treatment, the maximum production of acetic and oxalic acid was always reached earlier than for the ER-EF treatment. It is necessary to point out that a small amount of chloroacetic acid was detected in the case of the EF pretreatment, but was never observed during the ER-EF treatment. Chloroacetic acid has been classified as priority pollutant in environment because of its phytotoxic and carcinogenic effect and its Predicted Natural Environmental Concentration in water is about 0.58 μg L^{-1} [53]. Finally, in the ER-EF treatment, a slower mineralization, a higher amount of small organic acids, and the absence of chlorinated intermediates can explain the higher biodegradability observed during the electrolysis.

3.3.3. Energy consumption

According to these results, alachlor degradation can be achieved by different processes. Firstly, electro-Fenton treatment alone is able to degrade alachlor with a mineralization yield of 92% after 3h and a concentration of Cl^- ions around 95% of the chlorine content of alachlor. This process requires a charge of 2160 C to treat 12.5 mg of alachlor (173 kC/g of alachlor), corresponding to a consumed energy of about 48 kWh/kg of alachlor for a difference of potential around 1 V. Secondly, a coupling between electro-Fenton and a biological treatment is also possible if the solution is biodegradable with $BOD_5/COD > 0.4$. This is achieved after 0.5 h of EF treatment of the solution^{alachlor} (Table 1). The charge is then 29 kC/g of alachlor and the energy consumed is 8 kWh/kg of alachlor, underlining the

Accepted manuscript

possible interest of the coupling process compared with EF treatment alone. Finally, the coupling between the ER-EF pretreatment and a biological process can also be envisaged. Since the BOD_5/COD ratio is 0.16 after only 0.25 h of EF treatment on solution$^{alachlor-ER}$, an increase of the biodegradability can be expected between 0.25 h and 0.5 h of electrolysis, as experimentally confirmed (Table 1). A charge of 2 kC/g of alachlor corresponding to an energy of 1.6 kWh/kg of alachlor is consumed to do the electroreduction of alachlor since the current efficiency has been previously estimated to be about 36 % [27]. Thus, ER-EF pretreatment could be interesting if the total energy that it consumed is lower than 29 kC/g alachlor, which corresponds to a time of 28 min for the EF treatment in these operating conditions. Thus, if the time of the electro-Fenton process is reduced by only 2 min, in these operating conditions, the ER-EF pretreatment begins to be less energy-consuming, owing to the higher energy consumption of EF compared with ER. However, these calculus were made on the basis of experiments performed at lab scale and without taking into account the price of the electrode material for example. Therefore, it is difficult to conclude on the interest of ER-EF pretreament for alachlor degradation in these conditions. This strategy should be assessed at higher scale to confirm its relevance.

4. Conclusions

The sequential ER and EF processes as pretreatment prior to biological treatment toward decontamination of alachlor were presented and compared to EF pretreatment alone. The EF pretreatment was performed in galvanostatic mode on graphite felt cathode with air feeding to promote the generation of H_2O_2 through two-electron reduction. Complete degradation and over 91% mineralization were achieved within 3 h EF oxidation after optimization of the current, the ferrous ions concentration and the air flow rate. The pseudo-first order kinetic model can well describe the alachlor degradation through the EF process. The radicals, including •OH, $•O_2^-$ and $•SO_4^-$, were the main reactive oxidants in this EF treatment, especially •OH with about 63% contribution to alachlor mineralization. The analysis of the intermediate products after EF oxidation of alachlor and the electroreduced solution allowed proposing similar mechanisms for the degradation of alachlor and deschloroalachlor, the main by-product of electroreduction. It showed that the presence of a chlorine atom in the molecule did not change the sites of the radical attack.

Accepted manuscript

Biodegradability improvement was shown on the basis of the BOD_5/COD ratio for EF and ER-EF processes. The lower BOD_5/COD ratio observed at the beginning of the EF treatment (<0.5h) can be attributed to the presence of organo-chloride compounds since the Cl^- ions concentration remained still low. The slower mineralization and the higher content in low-molecular weight organic acids found in the case of the ER-EF treatment were in favor of microbial growth and can explain the higher biodegradability observed after 0.5h of treatment. The presence of residual organo-chloride compounds such as chloroacetic acid identified during the EF process would also have an effect on the BOD_5/COD ratio. A comparison of the energy consumption of the different processes underlines the possible interest of coupling the electrochemical pretreatment (electro-Fenton or electroreduction followed by electro-Fenton) with a biological treatment, but further studies especially at pilot scale are necessary to be able to conclude on this point.

References

[1] Y. Qin, F. Song, Z. Ai, P. Zhang, L. Zhang, Protocatechuic acid promoted alachlor degradation in Fe (III)/H2O2 Fenton system, Environmental Science & Technology, 49 (2015) 7948-7956.

[2] D.L. Carlson, M.M. McGuire, A.L. Roberts, D.H. Fairbrother, Influence of surface composition on the kinetics of alachlor reduction by iron pyrite, Environmental science & technology, 37 (2003) 2394-2399.

[3] M.H. Pérez, L.P. Vega, H. Zúñiga-Benítez, G.A. Peñuela, Comparative Degradation of Alachlor Using Photocatalysis and Photo-Fenton, Water, Air, & Soil Pollution, 229 (2018) 346.

Accepted manuscript

[4] C. Chevrier, T. Serrano, R. Lecerf, G. Limon, C. Petit, C. Monfort, L. Hubert-Moy, G. Durand, S. Cordier, Environmental determinants of the urinary concentrations of herbicides during pregnancy: The PELAGIE mother–child cohort (France), Environment International, 63 (2014) 11-18.

[5] H. Lee, J.-H. Kim, E. Kim, Y. Shin, J.-H. Lee, H. Jung, Y. Lim, H.S. Lee, J.-H. Kim, Biotransformation and molecular docking of cyazofamid by human liver microsomes and cDNA-expressed human recombinant P450s, Applied Biological Chemistry, 59 (2016) 649-653.

[6] P.A.E. Environmental, National primary drinking water regulations: Long Term 1 Enhanced Surface Water Treatment Rule. Final rule, Federal register, 67 (2002) 1811.

[7] J.-H. Zhu, X.-L. Yan, Y. Liu, B. Zhang, Improving alachlor biodegradability by ferrate oxidation, Journal of hazardous materials, 135 (2006) 94-99.

[8] G. Chen, Z. Wang, D. Xia, Electrochemically codeposited palladium/molybdenum oxide electrode for electrocatalytic reductive dechlorination of 4-chlorophenol, Electrochemistry communications, 6 (2004) 268-272.

[9] J.-M. Fontmorin, W. He, D. Floner, F. Fourcade, A. Amrane, F. Geneste, Reductive dehalogenation of 1, 3-dichloropropane by a [Ni (tetramethylcyclam)] Br2-Nafion® modified electrode, Electrochimica Acta, 137 (2014) 511-517.

[10] M.Á. Arellano-González, I. González, A.-C. Texier, Mineralization of 2-chlorophenol by sequential electrochemical reductive dechlorination and biological processes, Journal of hazardous materials, 314 (2016) 181-187.

[11] W. He, J.-M. Fontmorin, I. Soutrel, D. Floner, F. Fourcade, A. Amrane, F. Geneste, Reductive dechlorination of a chloroacetanilide herbicide in water by a Co complex-supported catalyst, Molecular Catalysis, 432 (2017) 8-14.

[12] W. He, J.-M. Fontmorin, P. Hapiot, I. Soutrel, D. Floner, F. Fourcade, A. Amrane, F. Geneste, A new bipyridyl cobalt complex for reductive dechlorination of pesticides, Electrochimica Acta, 207 (2016) 313-320.

[13] E. Verlato, W. He, A. Amrane, S. Barison, D. Floner, F. Fourcade, F. Geneste, M. Musiani, R. Seraglia, Preparation of Silver‐Modified Nickel Foams by Galvanic Displacement and Their Use as Cathodes for the Reductive Dechlorination of Herbicides, ChemElectroChem, 3 (2016) 2084-2092.

[14] W. He, Y. Lou, E. Verlato, I. Soutrel, D. Floner, F. Fourcade, A. Amrane, M. Musiani, F. Geneste, Reductive dehalogenation of a chloroacetanilide herbicide in a flow electrochemical cell fitted with Ag‐modified Ni foams, Journal of Chemical Technology & Biotechnology, 93 (2018) 1572-1578.

[15] J. Zhang, J.-W. Zheng, B. Liang, C.-H. Wang, S. Cai, Y.-Y. Ni, J. He, S.-P. Li, Biodegradation of Chloroacetamide Herbicides by Paracoccus sp. FLY-8 in Vitro, Journal of Agricultural and Food Chemistry, 59 (2011) 4614-4621.

Accepted manuscript

[16] H. Katsumata, S. Kaneco, T. Suzuki, K. Ohta, Y. Yobiko, Photo-Fenton degradation of alachlor in the presence of citrate solution, Journal of Photochemistry and Photobiology A: Chemistry, 180 (2006) 38-45.

[17] C. Wang, Z. Liu, Degradation of alachlor using an enhanced sono-Fenton process with efficient Fenton's reagent dosages, Journal of Environmental Science and Health, Part B, 50 (2015) 504-513.

[18] Z. Qiang, C. Liu, B. Dong, Y. Zhang, Degradation mechanism of alachlor during direct ozonation and O3/H2O2 advanced oxidation process, Chemosphere, 78 (2010) 517-526.

[19] D. Zheng, Y. Xin, D. Ma, X. Wang, J. Wu, M. Gao, Preparation of graphene/TiO 2 nanotube array photoelectrodes and their photocatalytic activity for the degradation of alachlor, Catalysis Science & Technology, 6 (2016) 1892-1902.

[20] Y.P. Bhoi, B. Mishra, Photocatalytic degradation of alachlor using type-II CuS/BiFeO3 heterojunctions as novel photocatalyst under visible light irradiation, Chemical Engineering Journal, 344 (2018) 391-401.

[21] A.R. Pipi, A.R. De Andrade, E. Brillas, I. Sires, Total removal of alachlor from water by electrochemical processes, Separation and Purification Technology, 132 (2014) 674-683.

[22] E. Chamarro, A. Marco, S. Esplugas, Use of Fenton reagent to improve organic chemical biodegradability, Water research, 35 (2001) 1047-1051.

[23] D. Mansour, F. Fourcade, I. Soutrel, D. Hauchard, N. Bellakhal, A. Amrane, Mineralization of synthetic and industrial pharmaceutical effluent containing trimethoprim by combining electro-Fenton and activated sludge treatment, Journal of the Taiwan institute of chemical engineers, 53 (2015) 58-67.

[24] A.A. Dalle, L. Domergue, F. Fourcade, A.A. Assadi, H. Djelal, T. Lendormi, I. Soutrel, S. Taha, A. Amrane, Efficiency of DMSO as hydroxyl radical probe in an Electrochemical Advanced Oxidation Process− Reactive oxygen species monitoring and impact of the current density, Electrochimica Acta, 246 (2017) 1-8.

[25] A. Aboudalle, F. Fourcade, A.A. Assadi, L. Domergue, H. Djelal, T. Lendormi, S. Taha, A. Amrane, Reactive oxygen and iron species monitoring to investigate the electro-Fenton performances. Impact of the electrochemical process on the biodegradability of metronidazole and its by-products, Chemosphere, 199 (2018) 486-494.

[26] R.J. Bigda, Consider Fentons chemistry for wastewater treatment, Chemical Engineering Progress, 91 (1995).

[27] Y. Lou, W. He, E. Verlato, Ni-coated graphite felt modified with Ag nanoparticles: a new electrode material for electro-reductive dechlorination, J. Electroanal. Chem., to be published.

[28] E. Brillas, I. Sirés, M.A. Oturan, Electro-Fenton process and related electrochemical technologies based on Fenton's reaction chemistry, Chemical reviews, 109 (2009) 6570-6631.

Accepted manuscript

[29] F. Ferrag - Siagh, F. Fourcade, I. Soutrel, H. Aït - Amar, H. Djelal, A. Amrane, Tetracycline degradation and mineralization by the coupling of an electro - Fenton pretreatment and a biological process, Journal of Chemical Technology & Biotechnology, 88 (2013) 1380-1386.

[30] Y. Lou, X. Ye, Z.-L. Ye, P.-C. Chiang, S. Chen, Occurrence and ecological risks of veterinary antibiotics in struvite recovered from swine wastewater, Journal of Cleaner Production, 201 (2018) 678-685.

[31] N.V. Klassen, D. Marchington, H.C. McGowan, H2O2 determination by the I3-method and by KMnO4 titration, Analytical Chemistry, 66 (1994) 2921-2925.

[32] F.C. Moreira, R.A. Boaventura, E. Brillas, V.J. Vilar, Electrochemical advanced oxidation processes: a review on their application to synthetic and real wastewaters, Applied Catalysis B: Environmental, 202 (2017) 217-261.

[33] Z. Qiang, J.-H. Chang, C.-P. Huang, Electrochemical generation of hydrogen peroxide from dissolved oxygen in acidic solutions, Water Research, 36 (2002) 85-94.

[34] S. Rezgui, A. Amrane, F. Fourcade, A. Assadi, L. Monser, N. Adhoum, Electro-Fenton catalyzed with magnetic chitosan beads for the removal of Chlordimeform insecticide, Applied Catalysis B: Environmental, (2017).

[35] J.R. Steter, E. Brillas, I. Sirés, On the selection of the anode material for the electrochemical removal of methylparaben from different aqueous media, Electrochimica Acta, 222 (2016) 1464-1474.

[36] G. Coria, I. Sirés, E. Brillas, J.L. Nava, Influence of the anode material on the degradation of naproxen by Fenton-based electrochemical processes, Chemical Engineering Journal, 304 (2016) 817-825.

[37] W. Zhou, J. Gao, K. Kou, X. Meng, Y. Wang, Y. Ding, Y. Xu, H. Zhao, S. Wu, Y. Qin, Highly efficient H2O2 electrogeneration from O2 reduction by pulsed current: Facilitated release of H2O2 from porous cathode to bulk, Journal of the Taiwan Institute of Chemical Engineers, 83 (2018) 59-63.

[38] W. Zhou, L. Rajic, L. Chen, K. Kou, Y. Ding, X. Meng, Y. Wang, B. Mulaw, J. Gao, Y. Qin, Activated carbon as effective cathode material in iron-free Electro-Fenton process: Integrated H2O2 electrogeneration, activation, and pollutants adsorption, Electrochimica acta, 296 (2019) 317-326.

[39] I. Sirés, E. Brillas, M.A. Oturan, M.A. Rodrigo, M. Panizza, Electrochemical advanced oxidation processes: today and tomorrow. A review, Environmental Science and Pollution Research, 21 (2014) 8336-8367.

[40] L. Zhou, Z. Hu, C. Zhang, Z. Bi, T. Jin, M. Zhou, Electrogeneration of hydrogen peroxide for electro-Fenton system by oxygen reduction using chemically modified graphite felt cathode, Separation and Purification Technology, 111 (2013) 131-136.

Accepted manuscript

[41] I. Sirés, J.A. Garrido, R.M. Rodríguez, E. Brillas, N. Oturan, M.A. Oturan, Catalytic behavior of the Fe3+/Fe2+ system in the electro-Fenton degradation of the antimicrobial chlorophene, Applied Catalysis B: Environmental, 72 (2007) 382-394.

[42] C. Annabi, F. Fourcade, I. Soutrel, F. Geneste, D. Floner, N. Bellakhal, A. Amrane, Degradation of enoxacin antibiotic by the electro-Fenton process: Optimization, biodegradability improvement and degradation mechanism, Journal of environmental management, 165 (2016) 96-105.

[43] M.V. Bagal, P.R. Gogate, Sonochemical degradation of alachlor in the presence of process intensifying additives, Separation and purification technology, 90 (2012) 92-100.

[44] W. Zhou, H. Zhao, J. Gao, X. Meng, S. Wu, Y. Qin, Influence of a reagents addition strategy on the Fenton oxidation of rhodamine B: control of the competitive reaction of·˙OH, RSC Advances, 6 (2016) 108791-108800.

[45] P. Vanraes, N. Wardenier, P. Surmont, F. Lynen, A. Nikiforov, S.W. Van Hulle, C. Leys, A. Bogaerts, Removal of alachlor, diuron and isoproturon in water in a falling film dielectric barrier discharge (DBD) reactor combined with adsorption on activated carbon textile: Reaction mechanisms and oxidation by-products, Journal of hazardous materials, 354 (2018) 180-190.

[46] W. Liu, Y. Wang, Z. Ai, L. Zhang, Hydrothermal synthesis of FeS2 as a high-efficiency Fenton reagent to degrade alachlor via superoxide-mediated Fe (II)/Fe (III) cycle, ACS applied materials & interfaces, 7 (2015) 28534-28544.

[47] M.L. Hladik, A.L. Roberts, E.J. Bouwer, Removal of neutral chloroacetamide herbicide degradates during simulated unit processes for drinking water treatment, Water research, 39 (2005) 5033-5044.

[48] S. Yahiat, F. Fourcade, S. Brosillon, A. Amrane, Photocatalysis as a pre-treatment prior to a biological degradation of cyproconazole, Desalination, 281 (2011) 61-67.

[49] P. Nidheesh, R. Gandhimathi, S. Velmathi, N. Sanjini, Magnetite as a heterogeneous electro Fenton catalyst for the removal of Rhodamine B from aqueous solution, Rsc Advances, 4 (2014) 5698-5708.

[50] C. Zhang, Y. Dong, B. Li, F. Li, Comparative study of three solid oxidants as substitutes of H2O2 used in Fe (III)-oxalate complex mediated Fenton system for photocatalytic elimination of reactive azo dye, Journal of Cleaner Production, 177 (2018) 245-253.

[51] V. Sarria, S. Parra, N. Adler, P. Péringer, N. Benitez, C. Pulgarín, Recent developments in the coupling of photoassisted and aerobic biological processes for the treatment of biorecalcitrant compounds, Catalysis Today, 76 (2002) 301-315.

[52] S. Randazzo, O. Scialdone, E. Brillas, I. Sirés, Comparative electrochemical treatments of two chlorinated aliphatic hydrocarbons. Time course of the main reaction by-products, Journal of hazardous materials, 192 (2011) 1555-1564.

Accepted manuscript

[53] A. Llort Sala, Degradation of Monochloroacetic acid by aluminium modified Fenton process, in, Universitat Politècnica de Catalunya, 2017.

Accepted manuscript

Figure legends

Figure 1. Effect of the applied cathodic current on the (a) generation of H_2O_2, (b) alachlor degradation, (c) mineralization. Experimental conditions: C_0(alachlor)=50 mg L^{-1}, [Fe(II)]=0.1 mmol L^{-1}, air flow rate=0.3 L min^{-1}, pH=3.0, [Na_2SO_4]=100 mmol L^{-1}, V=250 mL.

Figure 2. Effect of [Fe(II)] on (a) alachlor degradation and (b) mineralization. Experimental conditions: C_0(alachlor) = 50 mg L^{-1}, applied current = -200 mA, air flow rate = 0.3 L min^{-1}, pH = 3.0, [Na_2SO_4] = 100 mmol L^{-1}, V = 250 mL.

Figure 3. Effect of the air flow rate on (a) the generation of H_2O_2, (b) alachlor degradation, (c) mineralization. Experimental conditions: C_0(alachlor)=50 mg L^{-1}, applied current = -200 mA, [Fe(II)] = 0.05 mmol L^{-1}, pH = 3.0, [Na_2SO_4] = 100 mmol L^{-1}, V = 250 mL.

Figure 4. Proposed pathways for alachlor degradation by EF oxidation

Figure 5. Proposed pathways for deschloroalachlor degradation by EF oxidation

Figure 6. Time-course of the concentrations of Cl^-, NH_4^+ and NO_3^- during alachlor degradation by EF treatment. Experimental conditions: C_0(alachlor)=50 mg L^{-1}, applied current intensity = -200 mA, [Fe(II)] = 0.05 mmol L^{-1}, pH = 3.0, air flow rate=0.3 L min^{-1}, [Na_2SO_4] = 100 mmol L^{-1}, V = 250 mL

Figure 7. Effect of scavengers on alachlor conversion performance, [IPA]=2.50 mol L^{-1}, [TBA]=2.00 mol L^{-1}, [BQ]=20.0 mmol L^{-1}. The concentrations of different scavengers were referring Zhang et al. (2018). Experimental conditions: C_0(alachlor)=50 mg L^{-1}, applied current = -200 mA, [Fe(II)] = 0.05 mmol L^{-1}, pH = 3.0, air flow rate=0.3 L min^{-1}, [Na_2SO_4] = 100 mmol L^{-1}, V = 250 mL.

Figure 8. a) Dechlorination yield and b) Concentration of acetic acid (red square □), formic acid (blue cycle ○), and oxalic acid (green triangle Δ) during the EF treatment (dash line and open symbols) and the ER-EF treatment (solid line and symbols).

Table

Time (h)	TOC (mg L^{-1})	COD (mg O_2 L^{-1})	BOD_5 (mg O_2 L^{-1})	BOD_5/COD
solution^{alachlor}				
0	35.0 (±0.1)	105 (±0)	--	--
0.25	--	77 (±1)	--	--
0.5	21.7 (±0.7)	58 (±1)	223 (±4)	0.39 (±0.05)
1	15 (±2)	48 (±0)	31 (±0)	0.65 (±0.00)
1.5	9.3 (±0.1)	43 (±2)	26 (±4)	0.60 (±0.05)
2	6.1 (±0.9)	29 (±1)	13 (±4)	0.4 (±0.1)
solution$^{alachlor\text{-}ER}$				
0	30 (±2)	102 (±2)	--	--
0.25	--	74 (±1)	11.8 (±2)	0.16 (±0.03)

Accepted manuscript

0.5	23.5 (±0.8)	68 (±0)	26 (±2)	0.38 (±0.03)
1	19 (±1)	66.5 (±1)	47 (±2)	0.70 (±0.02)
1.5	14 (±2)	57 (±1)	39 (±2)	0.68 (±0.02)
2	10 (±2)	42 (±2)	26.5 (±0.7)	0.64 (±0.05)

Table 1. Biodegradability of by-products from EF and ER-EF treatments. Experimental conditions: C_0(alachlor)=50 mg L^{-1}, applied current = -200 mA, [Fe(II)] = 0.05 mmol L^{-1}, pH = 3.0, air flow rate=0.3 L min^{-1}, [Na_2SO_4] = 100 mmol L^{-1}, V = 250 mL.

Fig 1a

Accepted manuscript

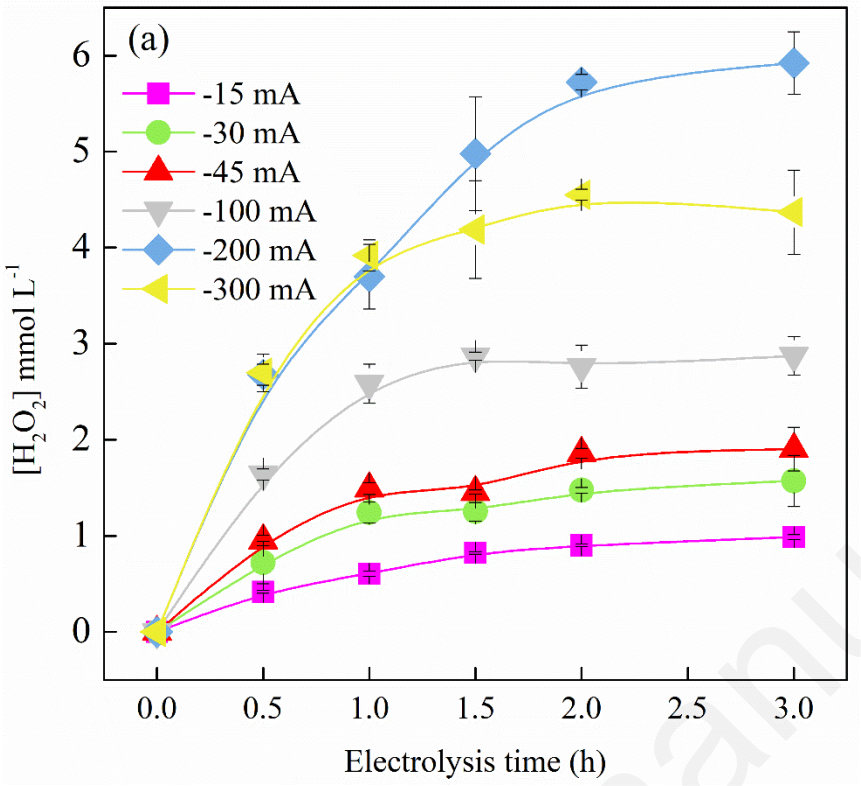

Fig 1b

Accepted manuscript

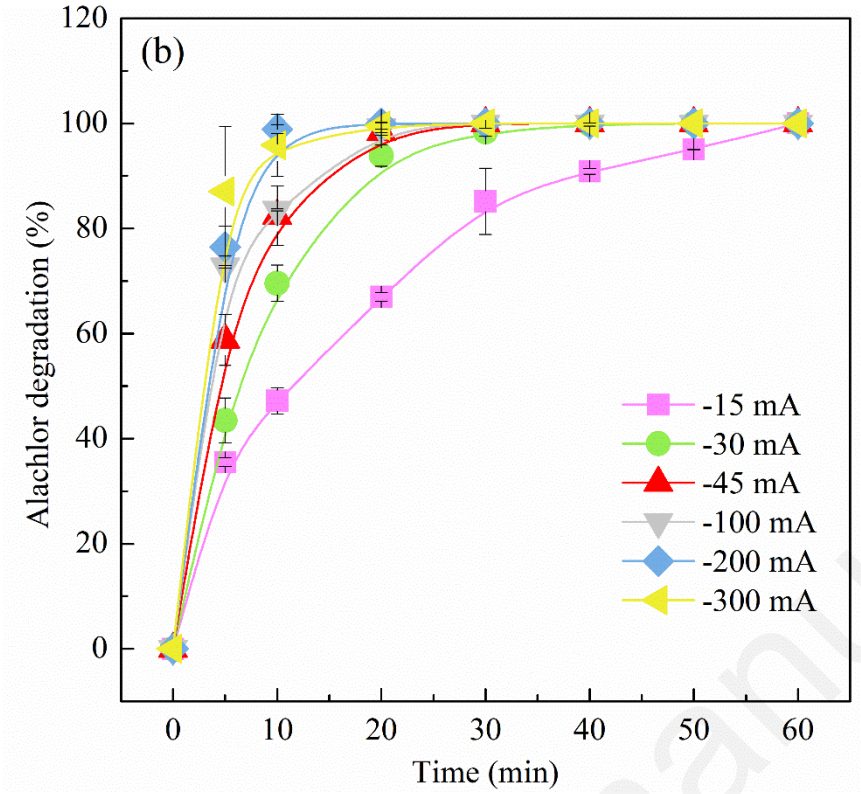

Fig 1c

Accepted manuscript

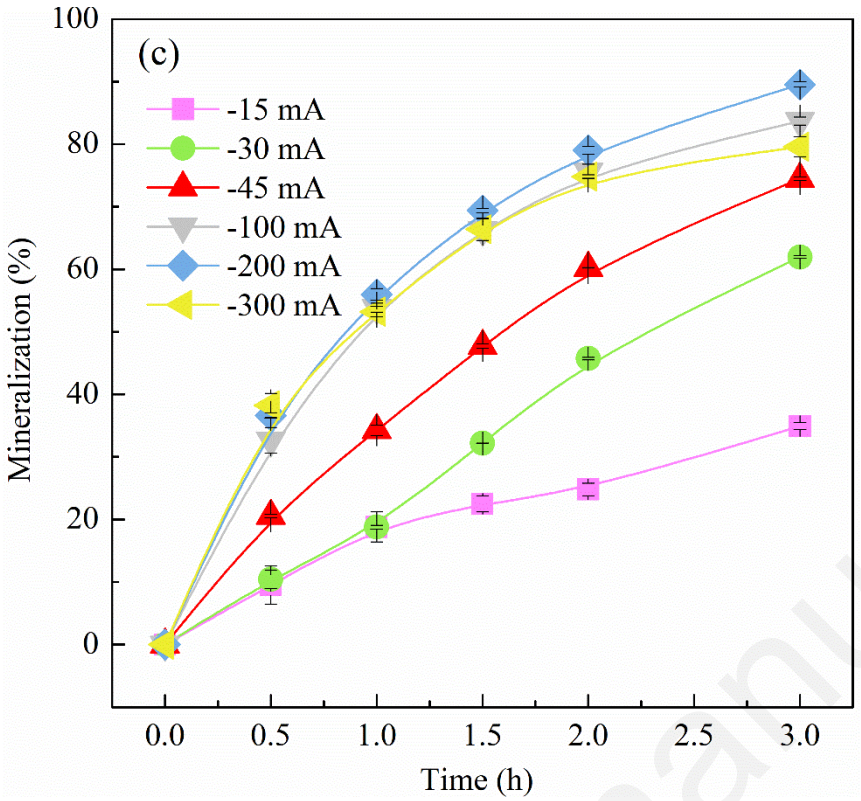

Fig 2a

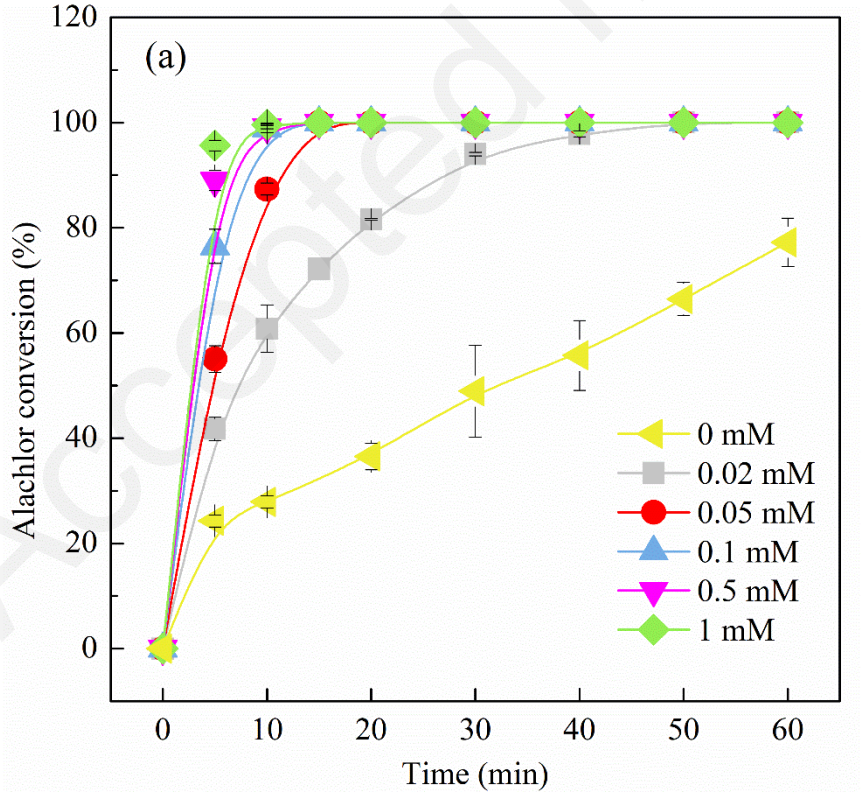

Accepted manuscript

Fig 2b

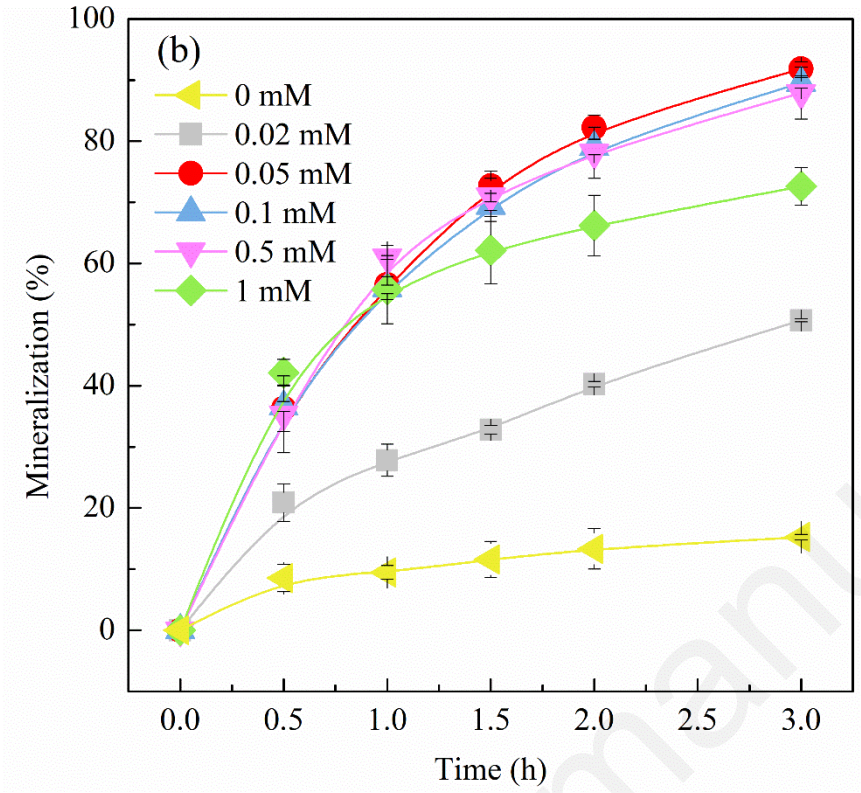

Fig 3a

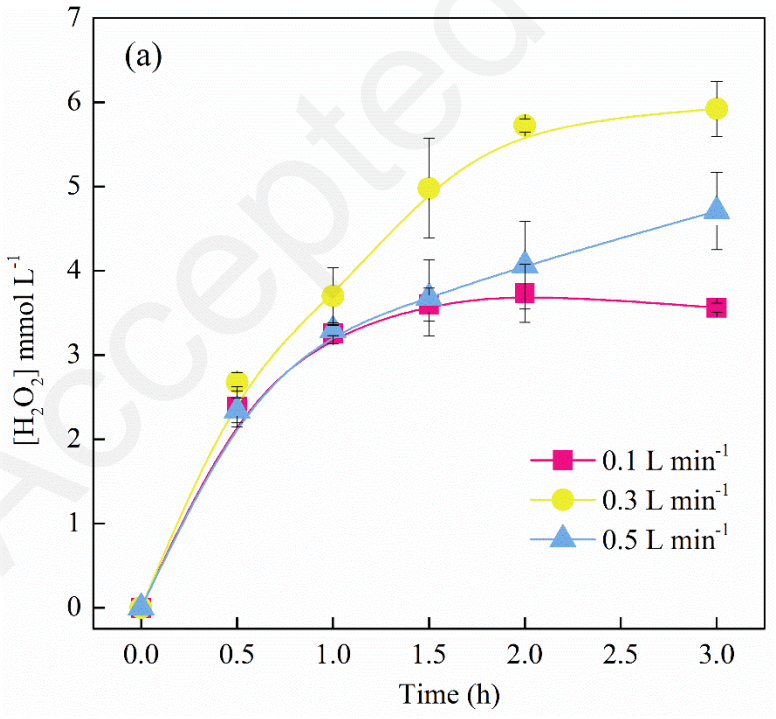

Accepted manuscript

Fig 3b

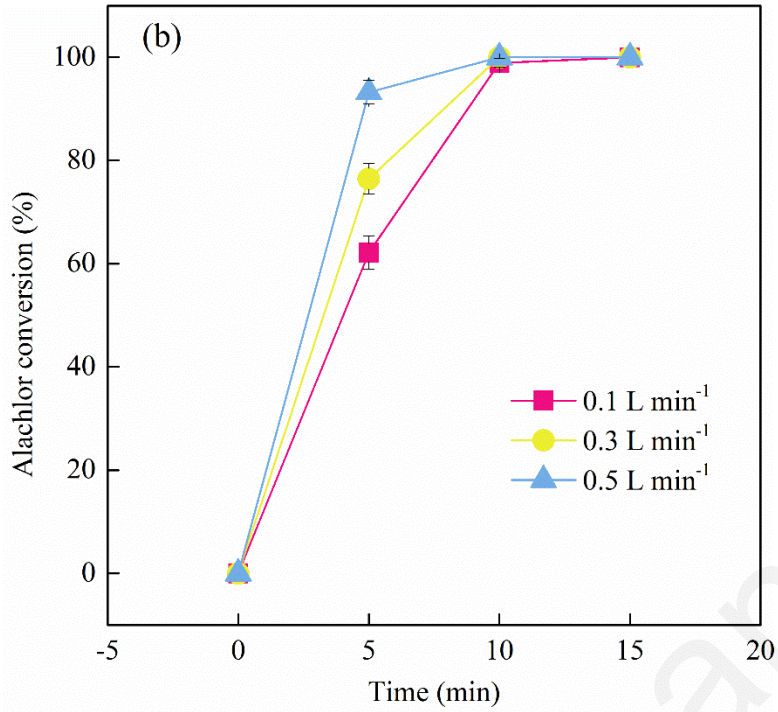

Fig 3c

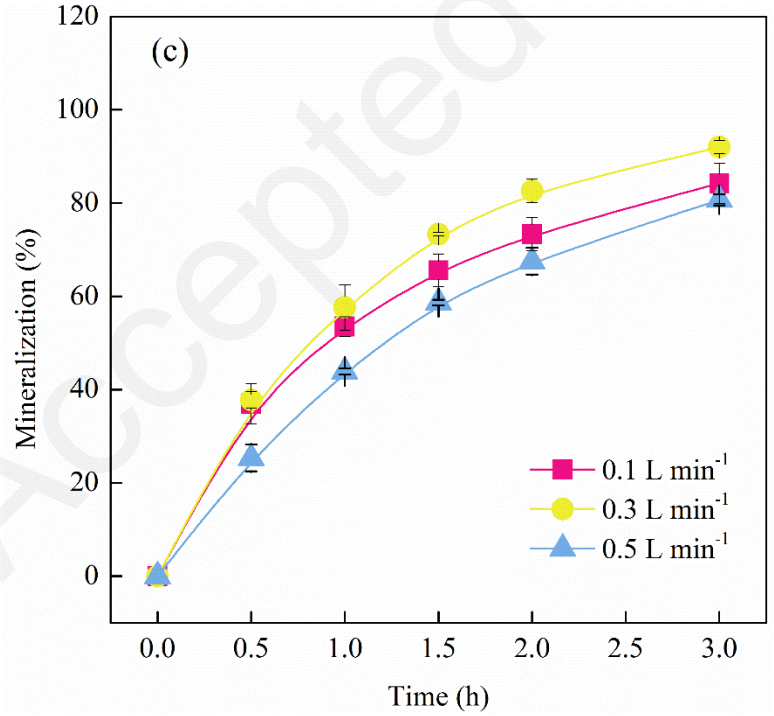

Accepted manuscript

Fig 4

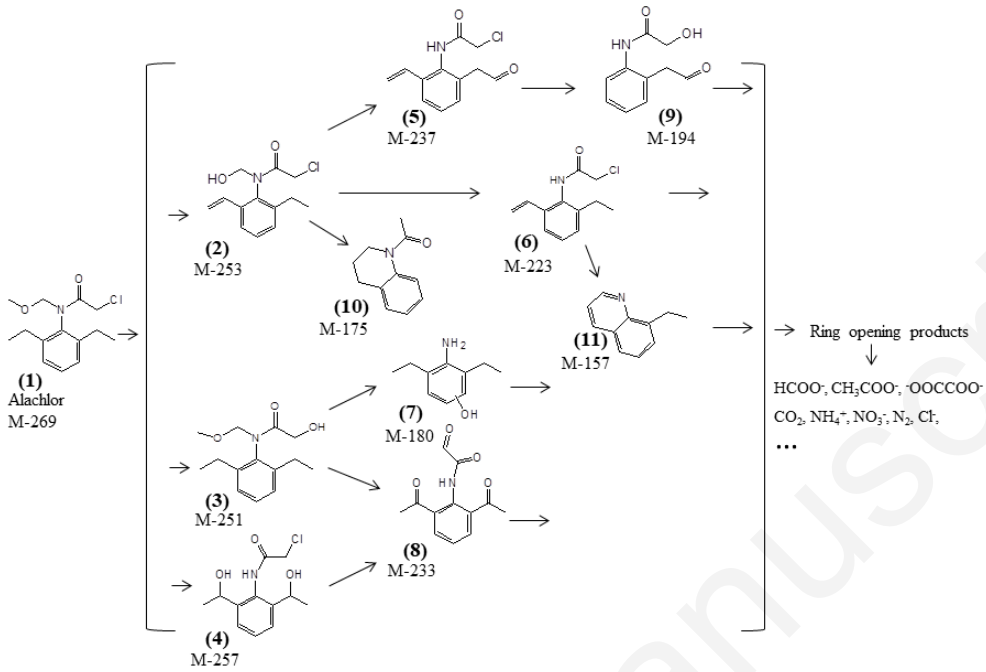

Fig 5

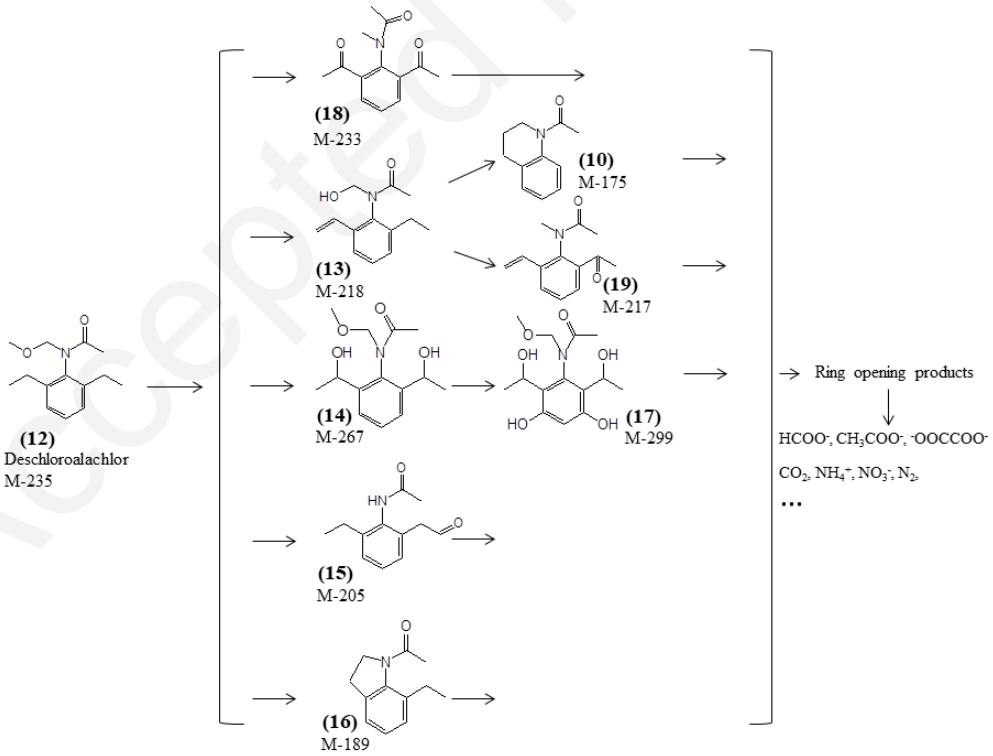

Accepted manuscript

Fig 6

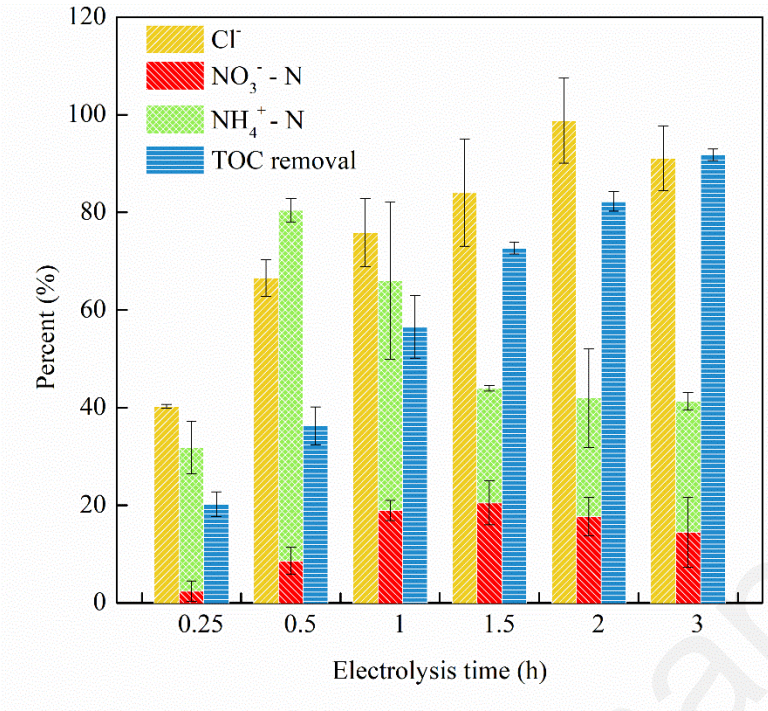

Fig 7

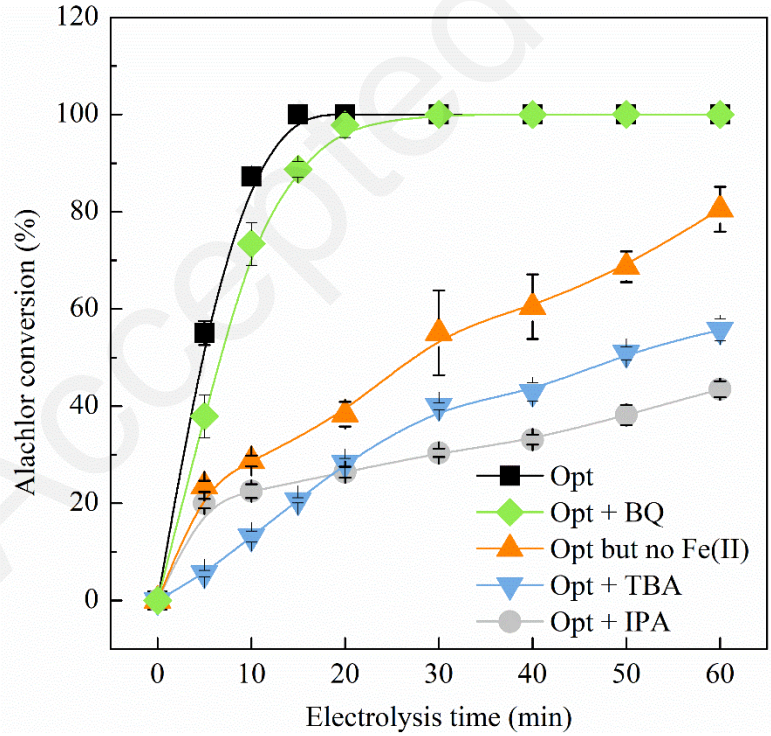

Accepted manuscript

Fig 8a

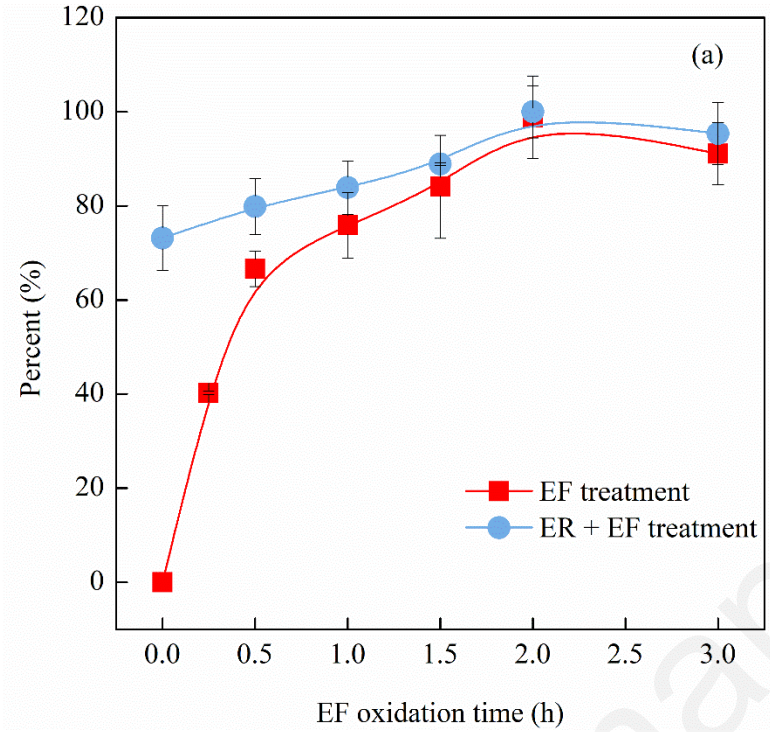

Fig 8b

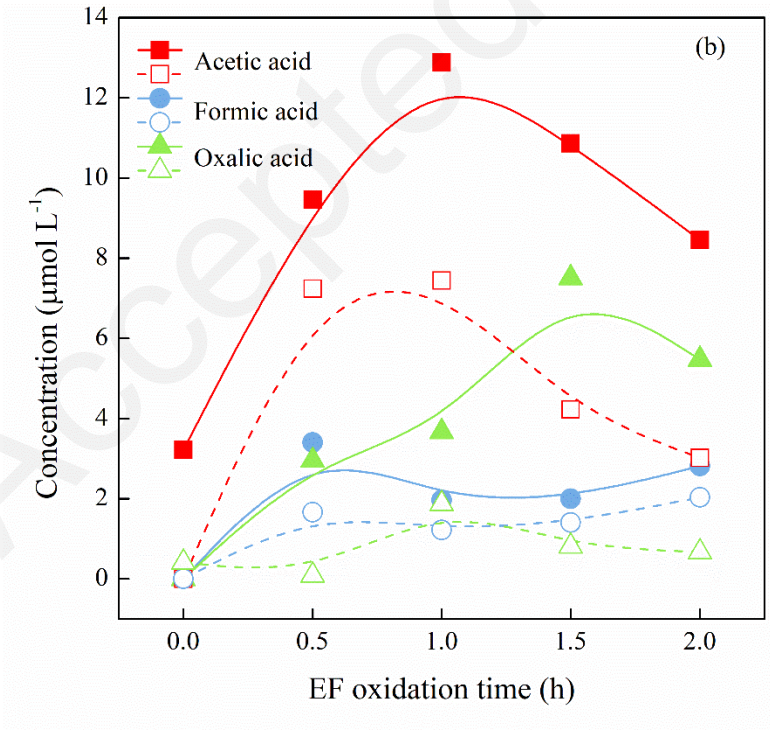

Accepted manuscript

Accepted manuscript